The Astrophysical Journal Letters, 814:L6 (6pp), 2015 November 20 doi:10.1088/2041-8205/814/1/L6

C III] EMISSION IN STAR-FORMING GALAXIES NEAR AND FAR

J. R. Rigby[1], M. B. Bayliss[2,3], M. D. Gladders[4,5], K. Sharon[6], E. Wuyts[7], H. Dahle[8], T. Johnson[6], and M. Peña-Guerrero[9]
[1] Astrophysics Science Division, Goddard Space Flight Center, 8800 Greenbelt Road, Greenbelt, MD 20771, USA
[2] Department of Physics, Harvard University, 17 Oxford Street, Cambridge, MA 02138, USA
[3] Harvard-Smithsonian Center for Astrophysics, 60 Garden Street, Cambridge, MA 02138, USA
[4] Department of Astronomy & Astrophysics, University of Chicago, 5640 S. Ellis Avenue, Chicago, IL 60637, USA
[5] Kavli Institute for Cosmological Physics, University of Chicago, 5640 South Ellis Avenue, Chicago, IL 60637, USA
[6] Department of Astronomy, University of Michigan, 500 Church Street, Ann Arbor, MI 48109, USA
[7] Max Plank Institute for Extraterrestrial Physics, Giessenbachstrasse 1, D-85748 Garching, Germany
[8] Institute of Theoretical Astrophysics, University of Oslo, P.O. Box 1029, Blindern, NO-0315 Oslo, Norway
[9] Space Telescope Science Institute, 3700 San Martin Drive, Baltimore, MD 21218, USA
Received 2015 September 11; accepted 2015 October 8; published 2015 November 13

ABSTRACT

We measure [C III] 1907, C III] 1909 Å emission lines in 11 gravitationally lensed star-forming galaxies at $z \sim 1.6$–3, finding much lower equivalent widths than previously reported for fainter lensed galaxies. While it is not yet clear what causes some galaxies to be strong C III] emitters, C III] emission is not a universal property of distant star-forming galaxies. We also examine C III] emission in 46 star-forming galaxies in the local universe, using archival spectra from GHRS, FOS, and STIS on *HST* and *IUE*. Twenty percent of these local galaxies show strong C III] emission, with equivalent widths < -5 Å. Three nearby galaxies show C III] emission equivalent widths as large as the most extreme emitters yet observed in the distant universe; all three are Wolf–Rayet galaxies. At all redshifts, strong C III] emission may pick out low-metallicity galaxies experiencing intense bursts of star formation. Such local C III] emitters may shed light on the conditions of star formation in certain extreme high-redshift galaxies.

Key words: galaxies: star formation – gravitational lensing: strong – techniques: spectroscopic

Supporting material: machine-readable table

1. INTRODUCTION

Rest-frame ultraviolet spectroscopy of star-forming $z \sim 2$–7 galaxies has revealed strong (rest-frame equivalent width $W_r < -5$ Å) emission lines of [C III] 1907, C III] 1909 Å (Shapley et al. 2003; Erb et al. 2010; Stark et al. 2014, 2015). Stark et al. (2014) suggest that C III] emission may be a way to spectroscopically confirm the highest-redshift galaxies. Such a tool would be particularly important if Lyα emission from galaxies at the reionization epoch is suppressed by neutral gas absorption (Pentericci et al. 2011, 2014; Treu et al. 2012, 2013; Caruana et al. 2013, 2014; Faisst et al. 2014; Tilvi et al. 2014). Such studies would need to understand selection effects—namely, the frequency of strong emission among star-forming galaxies.

There is a wide range in observed C III] equivalent widths at $z \sim 2$ (see Stark et al. 2014, Figure 3). It is not clear what physical conditions cause galaxies to produce strong equivalent width C III] emission; Stark et al. (2014) find that the emission line ratios of strong C III] emitters at $z \sim 2$ are consistent with low gas metallicity, a high ionization parameter, and a hard radiation field.

In addition, the C III] lines, together with lines of similar ionization potentials, namely, O III], N III], N IV], and Si III], can measure atomic abundances (see the study at $z = 3.6$ by Bayliss et al. 2014), and thus may be used to constrain nucleosynthetic yields in the early universe.

This Letter has three objectives. First, we measure C III] equivalent width in 11 gravitationally lensed galaxies at $z \sim 2$–3. This increases the published set of such measurements by a third, and explores a different parameter space than Stark et al. (2014), namely, higher stellar mass and metallicity. Second, we measure C III] equivalent widths for star-forming galaxies in the local universe. For nearby samples, it is easier to measure physical conditions, spatially resolve ionized regions, and test hypotheses for what produces strong C III] emission. Moreover, if strong C III] emission is a signature of primitive galaxies, then nearby galaxies with such emission should be investigated as analogs of high-redshift galaxies. Third, we explore the dependence of the C III] equivalent width on gas-phase metallicity.

2. DATA AND METHODS

Equivalent width measurements are in Table 1.

2.1. Measurements for Distant Galaxies

We measure the equivalent widths of Lyα and the C III] doublet in the rest-frame UV spectra of 11 gravitationally lensed galaxies at $1.6 < z < 3.1$. Spectra were obtained using the MagE spectrograph (Marshall et al. 2008) on the Clay Magellan II telescope, as part of a large study of the rest-frame ultraviolet spectral properties of bright lensed galaxies (J. R. Rigby et al. 2016, in preparation).

Intrinsic (corrected for lensing magnification) stellar masses and star formation rates have been published for three of these galaxies (Wuyts et al. 2012a) and are $(3–7) \times 10^9\, M_\odot$ and 20–100 $M_\odot\ \mathrm{yr}^{-1}$. Since final lensing models are in development for the MagE sample, we cannot yet quote stellar masses and star formation rates for the others. Metallicities from [N II]/Hα have been published for four of the sample galaxies: SGAS 090003.3+223408 (Bian et al. 2010), the Cosmic Horseshoe (Hainline et al. 2009), SGAS J152745.1+065219 (Wuyts et al. 2012a), and RCSGA 032727−132609 (hereafter RCS0327; Whitaker et al. 2014; Wuyts et al. 2014). We measure the metallicity for a fifth galaxy, SGAS J000451.7

Table 1
Galaxy Samples, Properties, and Equivalent Widths

Name	z	Z	Ref	W_r(Lyα) (Å)	σ (Å)	Ref	W_r(C III]) (Å)	σ (Å)	Ref	Sample	m_{AB}	Ref
RCSGA 032727 −132609 Knot E	1.703745	8.34 ± 0.02	W14	>−1.2	−99	R14	−2.0	0.14	R14	MagE	$g = 19.15$	W10
SGAS J000451.7–010321	1.6811	$8.30^{+0.06}_{-0.08}$	FIRE	−3.3	0.4	R14	−0.45	0.14	R14	MagE	$g = 19.91$	A09
Pox 120	0.020748	7.83	G96	−70.2	4.11	*IUE*	−14.4	1.8	*IUE*	G96	⋯	⋯
IRAS 08339+6517	0.019113	8.31	PG15	−4.45	0.5	STIS	−0.7	0.1	STIS	PG15	⋯	⋯
NGC 4861	0.002785	7.9	L11	⋯	⋯	⋯	−8.1	1.0	FOS	L11	⋯	⋯

Note. Columns: (1) source name; (2) redshift; (3) 12 + log(O/H) metallicity; (4) reference; (5) rest-frame Lyα equivalent width; (6) uncertainty; (7) reference; (8) rest-frame C III] equivalent width, sum of both transitions when resolved; (9) uncertainty; (10) reference; (11) sample; (12) magnitude for MagE sample; (13) reference. Redshifts for MagE galaxies are from Bordoloi et al. (2015) for RCS0327, else from Rigby et al. (2014) and in preparation. Redshifts for $z \sim 0$ galaxies are from NED.

References. A09—Abazajian et al. (2009), B07—Belokurov et al. (2007), B10—Bian et al. (2010), G96—Giavalisco et al. (1996), H09—Hainline et al. (2009), K10—Koester et al. (2010), L11—Leitherer et al. (2011), PG15—M. Peña-Guerrero et al. (2015, in preparation), R14—Rigby et al. (2014), S07—Smail et al. (2007), W10—Wuyts et al. (2010), W12—Wuyts et al. (2012b), W14—Wuyts et al. (2014).

(This table is available in its entirety in machine-readable form.)

−010321, from the [N II]/Hα ratio in FIRE/*Magellan* spectra. We use the second-order polynomial calibration of Pettini & Pagel (2004).

From the literature, we take C III] equivalent widths for six galaxies from Erb et al. (2010), Christensen et al. (2012), Stark et al. (2014), and Bayliss et al. (2014) with measured metallicities. Four galaxies have metallicities derived by Stark et al. (2014) using a Bayesian approach that relies on the strong emission lines used by the R_{23} method; the R_{23} metallicity measured by Christensen et al. (2012) for one of those galaxies agrees with the Bayesian method. Erb et al. (2010) measured an R_{23} metallicity for BX418 at $z = 2.30$, as did Bayliss et al. (2014) for SGAS J105039.6+001730 at $z = 3.625$.

2.2. Measurements for Nearby Galaxies

We take spectra of nearby galaxies from three spectral atlases: Leitherer et al. (2011), M. Peña-Guerrero et al. (2015, in preparation), and Giavalisco et al. (1996).

For 17 galaxies from Leitherer et al. (2011), we take metallicities from their tabulation and measurements of the C III] equivalent width from Bayliss et al. (2014). Four of these galaxies have spectra of multiple regions, totaling 27 measurements of C III]. Thirteen of these galaxies have archival *International Ultraviolet Explorer* (*IUE*) spectra that cover C III], many of which show C III] emission, even in favorable cases lines of moderate equivalent width, for example, IRAS 08339+6517. For the 18 galaxies of Peña-Guerrero et al. (2015, in preparation), we measure C III] equivalent widths from the *HST* spectra and take direct gas-phase metallicity measurements from their Table 9. For the 11 galaxies (out of 22) from Giavalisco et al. (1996) that have a continuum signal-to-noise ratio $\gtrsim 1\ \mathrm{pixel}^{-1}$, we measure equivalent widths from archival low dispersion (6 Å) *IUE* spectra.

We measure Lyα equivalent widths for the subset of those galaxies that have archival spectra covering Lyα and redshifts sufficient, given the spectral resolution of each spectrum, to cleanly separate in the galaxy's Lyα emission from the much brighter geocoronal Lyα emission (Biretta et al. 2015). These criteria are met for: Tol-1214–277 from Leitherer et al. (2011; *IUE* spectra); two galaxies from Peña-Guerrero et al. (2015, in preparation), IRAS 08339+6517 from *HST* and *IUE* spectra, and NGC 1741 from an *IUE* spectrum; and the 11 galaxies from Giavalisco et al. (1996; *IUE* spectra).

These are spectra from published atlases, not from a complete galaxy sample. Further, they were obtained using a range of aperture size: 10″ × 20″ with *IUE*, 1″–2″ with FOS and GHRS, and 0″.2 with STIS. As such, some observations capture bright star-forming regions within a galaxy, whereas others capture the integrated galaxy spectrum. These are necessary limitations of current ultraviolet spectroscopic atlases.

2.3. Uncertainties

When fitting equivalent widths of C III] and Lyα, our uncertainties incorporate statistical uncertainty as well as systematic uncertainty due to continuum estimation. Each reported equivalent width is the mean of measurements assuming a linear continuum, power-law continuum, and (if the spectrum is locally flat) median continuum. We take the standard deviation as the systematic uncertainty due to continuum fitting; it is typically less than half the measurement uncertainty.

The spectra analyzed here vary widely in resolution and signal-to-noise ratio, resulting in emission line equivalent width measurements ranging from strong to weak detections. For sources with strong emission lines and a weak or non-detected continuum, the measurement is a lower limit on the equivalent width; the associated uncertainty may be large even though the emission line is very well detected and reflects the continuum uncertainty.

Following the definition of equivalent width, equivalent widths have a positive sign for absorption and a negative sign for emission.

3. RESULTS

3.1. C III] Equivalent Width

We measure C III] strengths in bright lensed, star-forming galaxies at $z \sim 2$–4, as well as in local starbursting galaxies with archival ultraviolet spectra from *HST* and *IUE*. Figure 1 compares histograms of C III] equivalent width in these samples, as well as to Stark et al. (2014) and the composite spectrum of Shapley et al. (2003). Figure 1 demonstrates that

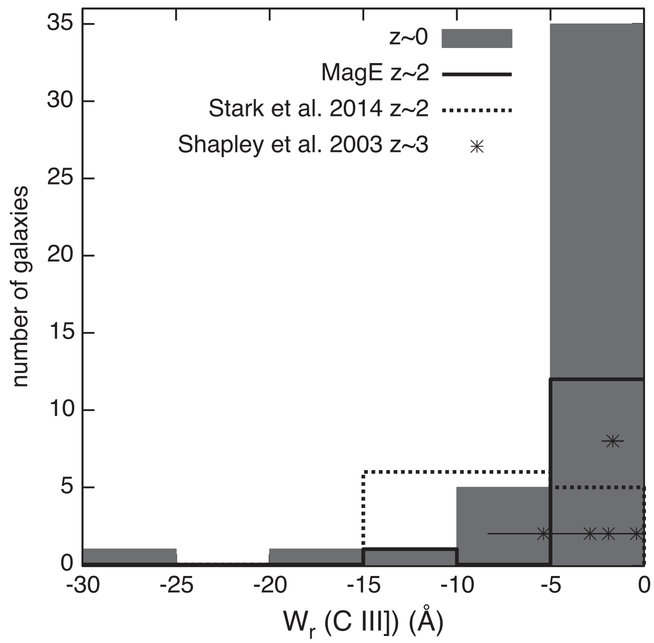

Figure 1. Histograms of [C III] 1907, C III] 1909 Å rest-frame equivalent width. The $z \sim 0$ sample (gray filled histogram) combines galaxies from Leitherer et al. (2011), Peña-Guerrero et al. (2015, in preparation), and Giavalisco et al. (1996). Two $z \sim 2$ samples are shown: the MagE spectral atlas (solid black line), including the $z = 3.6$ galaxy from Bayliss et al. (2014), and the galaxies from Stark et al. (2014; dashed black line.) Asterisks shows equivalent widths for the composite spectrum and composite quartile spectra of Shapley et al. (2003), with 1σ uncertainty, at arbitrary y values. At both $z \sim 0$ and $z \sim 2$, the mode is small, and there is a tail to large equivalent widths.

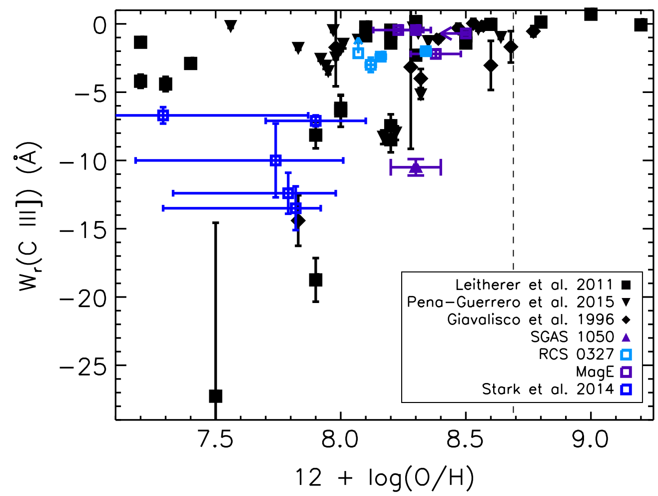

Figure 2. Rest-frame C III] equivalent width as a function of gas-phase metallicity. Nearby galaxies are plotted in black: Leitherer et al. (2011; black squares); the STIS sample of Peña-Guerrero et al. (2015, in preparation; black triangles); and Giavalisco et al. (1996; black diamonds). Redshift $z \sim 2$–4 galaxies are plotted with colored symbols: SGAS J105039.6+001730 at $z = 3.6$ (Bayliss et al. 2014; purple triangle); four physically distinct star-forming regions within lensed galaxy RCS0327 at $z = 1.70$ (light blue squares); four additional galaxies at $1.6 < z < 2.8$ with MagE spectra and measured metallicities (purple squares and upper limit); four galaxies from Stark et al. (2014) with measured metallicity; and one galaxy (BX418) from Erb et al. (2010; blue squares). A dashed line marks solar metallicity (Asplund et al. 2009). At large equivalent width, systematic uncertainty in the continuum level dominates. Metallicity appears to set an envelope; low metallicity may be a necessary but not sufficient condition for high C III] equivalent widths.

star-forming galaxies in the local universe and at $z \sim 2$–4 show a large range of C III] equivalent widths. The mode for the distant galaxies and the mode for the $z \sim 0$ galaxies are consistent with the equivalent width measured for the Shapley et al. (2003) composite. A significant minority of galaxies show strong C III] emission with Wr (C III]) < -5 Å: 22% of the $z \sim 0$ sample and 45% of the $z \sim 2$–4 sample.

Indeed, the local sample includes a tail of strong C III] emitters with equivalent widths to -25 Å, widths that are beyond that yet observed at $z \sim 2$. These results are consistent with a scenario in which strong C III] emission is not a particular feature of $z \gtrsim 2$ galaxies, but rather occurs in a minority of starbursting galaxies independent of redshift.

The MagE sample has systematically lower equivalent widths than the Stark et al. (2014) sample. The MagE sample galaxies were selected as lensed galaxies that are most amenable to deep rest-frame UV spectroscopy; they have typical apparent magnitudes of $g_{AB} \sim 20$–21 and should be biased toward high surface brightness, high magnification, high luminosity, and compact morphology. Wuyts et al. (2012a) examined in detail the spectral energy distributions of three galaxies from the MagE sample, finding them typical of Lyman break galaxies, though younger than average. By contrast, the Stark et al. (2014) sample is selected to be much fainter, with an average apparent V-band magnitude of $m_{AB} = 23.9$.

3.2. *C III] Equivalent Width as a Function of Metallicity*

Figure 2 plots the C III] equivalent width as a function of gas-phase metallicity for the $z \sim 0$ samples (black symbols) and the $z \sim 2$–4 samples (blue and purple symbols). Stark et al. (2014) suggest that low metallicity may be largely responsible for large equivalent widths. Figure 2 reveals that the relationship with metallicity is complex. Strong emission ($\lesssim -5$ Å) is observed in galaxies over a wide range of metallicity, from 6% to 40% of solar. Strong emission appears not to occur at metallicities above $12 + \log(O/H) = 8.4$. Indeed, only one of the six lowest-metallicity $z \sim 0$ galaxies shows strong emission. Thus, low metallicity may be a necessary but not sufficient condition for C III] emission.

3.3. *Strong C III] Emitters in the Local Universe*

Figure 2 demonstrates that the local universe contains galaxies whose C III] emission is as strong, indeed stronger, than yet observed at $z \sim 2$. The three galaxies from the $z \sim 0$ samples with the most extreme C III], with equivalent widths exceeding -14 Å, are Tololo 1214–277, Markarian 71 (a star-forming region within NGC 2366),[10] and Pox 120. We now explore what is known about these three galaxies and plot their ultraviolet spectra in Figure 3.

Tololo 1214–277 is classified as a Wolf–Rayet galaxy, Mrk 71 is classified as a star cluster containing Wolf–Rayet stars within the irregular galaxy NGC 2366, and Pox 120 is classified as a Wolf–Rayet galaxy (Kunth & Joubert 1985; Schaerer et al. 1999). The equivalent width of Hα is extremely high for Mrk 71 (< -1000Å; Buckalew et al. 2005) and for TOL 1214–277 (-1700 Å; Guseva et al. 2011). We could not find a published W_r(Hα) for Pox 120. Only 1 (15) of the 417 nearby galaxies of Moustakas & Kennicutt (2006) shows an Hα equivalent width of < -1000Å (< -200Å). Simple stellar populations with such high equivalent widths have ages of only

[10] Many studies incorrectly name this object; see http://cdsarc.u-strasbg.fr/viz-bin/vizExec/getpuz?7239&N%202363.

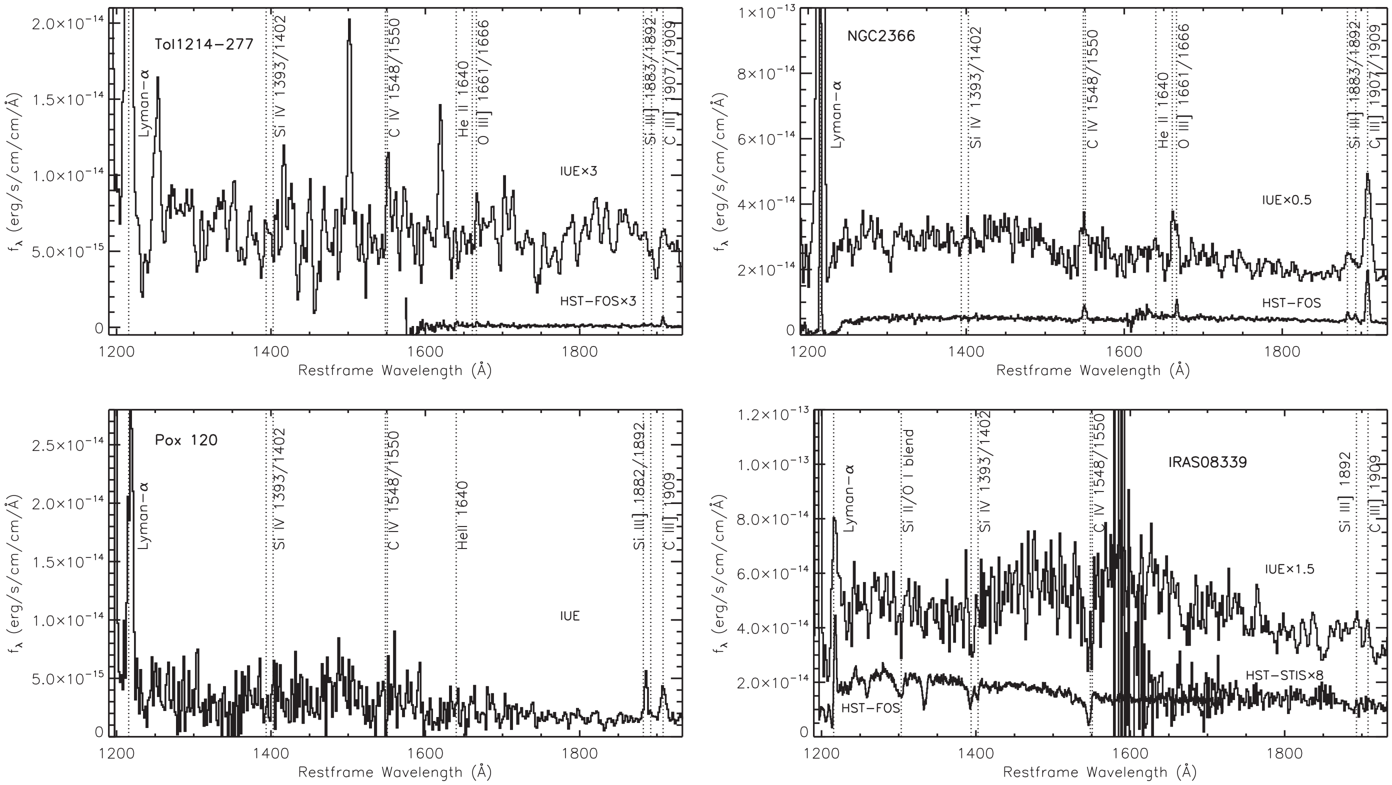

Figure 3. Spectra of C III] emitters at $z \sim 0$. The three $z = 0$ emitters with the largest W_r(C III]) are plotted: Tololo 1214–277 (top left), the region Mrk 71 within galaxy NGC 2366 (top right), and Pox 120 (bottom left). For comparison, we also plot a spectrum with moderate emission, IRAS 08339+6517 (bottom right). The W_r(C III]) for Tol-1214−277 is larger in *HST*-FOS compared to *IUE*, which we attribute to aperture effects. Clearly, low-redshift galaxies can produce strong C III] emission.

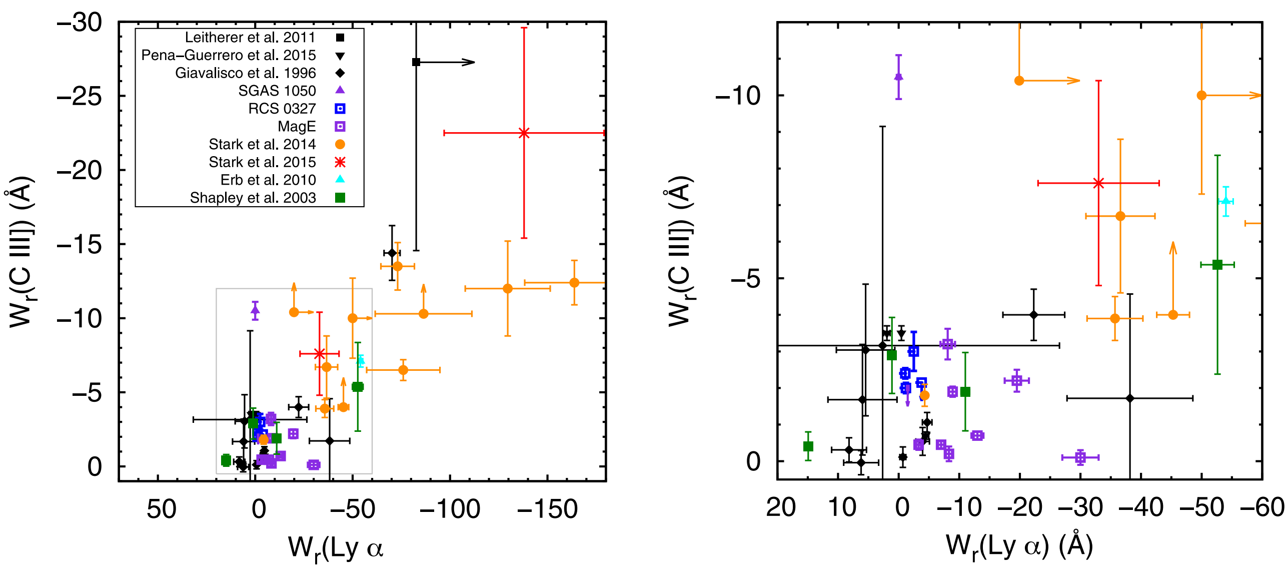

Figure 4. Left panel: comparison of rest-frame equivalent widths of Lyα and C III]. Nearby galaxies are plotted in black, and $1.6 < z < 7$ galaxies are plotted with other colors. Symbols are coded as in Figure 2, with additional values from Stark et al. (2014; orange circles), Stark et al. (2015; red asterisks), Erb et al. (2010); cyan triangle), and Shapley et al. (2003; green squares). Two *IUE* spectra were available for each of IRAS 08339+6517 and NGC 1741; we plot a point for each spectrum. Right panel: zoom of the region outlined in gray, containing most of our $z \sim 2$ MagE and $z \sim 0$ measurements. The equivalent widths are correlated, but the correlation is not obvious within the MagE sample.

a few million years (cf. Figure 23 of Leitherer et al. 2014.) Another indication of the extreme star formation occurring in these galaxies is the fact that Tololo 1214–277 is one of very few galaxies in the local universe that shows indications of leaking Lyman continuum photons (Verhamme et al. 2015).

In addition, 7 $z \sim 0$ galaxies show strong C III] emission with $-14 < W_r < -5$ Å. These are: NGC 5253 (regions HIIR-1 and HIIR-2), NGC 4861, NGC 5457 (region NGC 5471), Tololo 1345–420, Sbs 1319+579, III Zw 107, and Arp 252.

3.4. Lyα

Shapley et al. (2003) noted a correlation between the equivalent widths of C III] and Lyα emission in their quartile composite spectra. Stark et al. (2014, 2015) further examined this correlation. In Figure 4, we plot W_r(C III]) versus W_r(Lyα) for galaxies at $1.6 < z < 7$, as well as galaxies at $z \sim 0$. A correlation is apparent for both redshift ranges, though there is considerable scatter. The correlation is dominated by the strongest emitters, with $W(\mathrm{Ly}\alpha) \lesssim -50$ Å, $W(\mathrm{C\,III]}) \lesssim -5$ Å. Within the dynamic range of the MagE sample, no correlation is apparent.

3.5. Strongly Star-forming Galaxies that Are Not Strong C III] Emitters

Since the physical conditions of the lensed galaxy RCS0327 at $z = 1.70$ have been measured precisely, we compare them to the derived physical parameters of the Stark et al. (2014) sample. RCS0327 has a measured ionization parameter $\log U = -2.84 \pm 0.06$ (Rigby et al. 2011, using the average extinction from Whitaker et al. 2014.) This value is consistent with ionization parameters measured for other lensed Lyman break galaxies: SGAS J122651.3+215220 and SGAS J152745.1+065219 in the MagE sample (Wuyts et al. 2012a), the Cosmic Horseshoe and the Clone (Hainline et al. 2009), and cB58 (Pettini et al. 2002). The ionization parameters of these LBGs are 0.6–1 dex lower than those inferred by Stark et al. (2014) for four galaxies. RCS0327 has a measured stellar mass of $6.3 \pm 0.7 \times 10^9\,M_\odot$ and a star formation rate of 30–50 $M_\odot\,\mathrm{yr}^{-1}$ (Wuyts et al. 2012a). Its specific star formation rate (sSFR) is $5 \times 10^{-9}\,\mathrm{yr}^{-1}$, such that it lies a factor of 3 above the correlation between star formation rate and stellar mass at that redshift. Three objects in Stark et al. (2014) have lower sSFRs than this; all have very strong C III] emission with $W_r \leqslant -10$ Å. Of the four galaxies in Stark et al. (2014) with highest stellar mass, $8.9 < \log[M_*/M_\odot] < 9.2$, three have C III] equivalent widths <-4 Å. Thus, RCS0327 is similar to the Stark et al. (2014) sample in terms of sSFR, but has a higher metallicity and lower ionization parameter than inferred for that sample. This comparison provides some support for the hypothesis of Stark et al. (2014) that both low metallicity and a high ionization parameter are required to create strong C III] emission.

Perhaps more surprising is the fact that the vigorously star-forming, very low metallicity starburst galaxy 1 Zw 18 is *not* a strong C III] emitter; its equivalent width in three different regions varies from -1.3 to -4.4 Å. Its ionization parameter is high for the local universe ($\log U \sim -2.5$ from Dufour et al. 1988; inferred as -2.2 as the lowest-metallicity object in Morales-Luis et al. 2014). Any hypothesis that explains strong C III] emission will need to explain why 1 Zw 18 shows relatively weak C III] emission.

4. LOOKING FORWARD

C III] emission has emerged as a practical method to spectroscopically confirm galaxies at the reionization epoch should Lyα emission prove to be suppressed. Our MagE spectra of lensed $1.6 < z < 3$ star-forming galaxies show that C III] emission typically has a modest equivalent width in bright, high surface brightness galaxies at that epoch; this result is consistent with the composite spectra of Shapley et al. (2003). Strong C III] emission is clearly not a universal feature of galaxies at that epoch; equivalent widths exceeding -5 Å are seen in 45% of the $z \sim 2$–4 galaxies examined here.

We have examined C III] emission in local star-forming galaxies with archival *HST* spectra; a minority (22%) show strong C III] emission. Three of these nearby galaxies show C III] emission as strong or stronger (< -14 Å) than yet reported for any galaxy at $z \sim 2$. The distribution function of the equivalent width of C III] emission at any redshift may contain a tail toward very high equivalent widths; if so, by compiling spectra for 46 nearby galaxies, we have sampled this tail. The high equivalent width tail may be more populated at $z \sim 2$ than at $z \sim 0$, but determining this would require matched samples at both redshifts, which has not yet been done. The sample of Stark et al. (2014) clearly samples this tail of strong emission, while the MagE galaxies reported here do not.

The question then becomes, what physical conditions cause galaxies to be strong C III] emitters? For local galaxies, we see that metallicity may set an envelope on maximum C III] equivalent width. While low-metallicity galaxies show a wide range on C III] equivalent width, strong emission is only seen at low metallicity. Additional physical conditions must be required to produce strong C III] emission. The three $z \sim 0$ galaxies with extreme C III] emission, as strong as anything seen in the distant universe, are Wolf–Rayet galaxies with extremely high Hα equivalent widths. Such extreme emission calls to mind the candidate $z \sim 8$ dropout galaxies whose *Spitzer*/IRAC colors are best explained by extreme equivalent widths of [O III] $\lambda\lambda$4959,5007 and Hβ (Labbé et al. 2013). Follow-up investigations of these nearby, low-metallicity extreme C III] emitters may thus reveal the physical conditions that foster such strong emission from star-forming galaxies, with consequences for our understanding of star formation at the highest redshifts.

This Letter includes data gathered with the 6.5 m *Magellan* Telescopes located at Las Campanas Observatory, Chile. This research has made use of the NASA/IPAC Extragalactic Database (NED), which is operated by the Jet Propulsion Laboratory, California Institute of Technology, under contract with the National Aeronautics and Space Administration. This Letter includes observations made with the NASA/ESA *Hubble Space Telescope* and with the *International Ultraviolet Explorer*, obtained from the Data Archive at the Space Telescope Science Institute, which is operated by the Association of Universities for Research in Astronomy, Inc., under NASA contract NAS 5-26555. J.R. thanks the "First Carnegie Symposium in honor of Leonard Searle." We thank G. Sonneborn and S. Heap for advice regarding *IUE* spectra. H.D. acknowledges support from the Research Council of Norway.

REFERENCES

Abazajian, K. N., Adelman-McCarthy, J. K., Agüeros, M. A., et al. 2009, ApJS, 182, 543
Asplund, M., Grevesse, N., Sauval, A. J., & Scott, P. 2009, ARA&A, 47, 481
Bayliss, M. B., Rigby, J. R., Sharon, K., et al. 2014, ApJ, 790, 144
Belokurov, V., Evans, N. W., Moiseev, A., et al. 2007, ApJL, 671, L9
Bian, F., Fan, X., Bechtold, J., et al. 2010, ApJ, 725, 1877
Biretta, J., Aloisi, A., Bohlin, R., et al. 2015, STIS Instrument Handbook, Version 14.0 (Baltimore, MD: STScI)
Bordoloi, R., Rigby, J. R., Tumlinson, M. B., et al. 2015, MNRAS, submitted
Buckalew, B. A., Kobulnicky, H. A., & Dufour, R. J. 2005, ApJS, 157, 30
Caruana, J., Bunker, A. J., Wilkins, S. M., et al. 2013, MNRAS, 427, 3055
Caruana, J., Bunker, A. J., Wilkins, S. M., et al. 2014, MNRAS, 443, 2831

Christensen, L., Richard, J., Hjorth, J., et al. 2012, MNRAS, 427, 1953
Dufour, R. J., Garnett, D. R., & Shields, G. A. 1988, ApJ, 332, 752
Erb, D. K., Pettini, M., Shapley, A. E., et al. 2010, ApJ, 719, 1168
Faisst, A. L., Capak, P., Carollo, C. M., Scarlata, C., & Scoville, N. 2014, ApJ, 788, 87
Giavalisco, M., Koratkar, A., & Calzetti, D. 1996, ApJ, 466, 831
Guseva, N. G., Izotov, Y. I., Stasińska, G., et al. 2011, A&A, 529, 149
Hainline, K. N., Shapley, A. E., Kornei, K. A., et al. 2009, ApJ, 701, 52
Koester, B. P., Gladders, M. D., Hennawi, J. F., et al. 2010, ApJL, 723, L73
Kunth, D., & Joubert, M. 1985, A&A, 142, 411
Labbé, I., Oesch, P. A., Bouwens, R. J., et al. 2013, ApJL, 777, L19
Leitherer, C., Ekstrom, S., Meynet, G., et al. 2014, ApJS, 212, 14
Leitherer, C., Tremonti, C. A., Heckman, T. M., & Calzetti, D. 2011, AJ, 141, 37
Marshall, J. L., Burles, S., Thompson, I. B., et al. 2008, Proc. SPIE, 7014, 701454
Morales-Luis, A. B., Perez-Montero, E., Sánchez Almeida, J., & Muñoz-Tuñón, C. 2014, ApJ, 797, 81
Moustakas, J., & Kennicutt, R. C. 2006, ApJS, 164, 81
Pentericci, L., Fontana, A., Vanzella, E., et al. 2011, ApJ, 743, 132
Pentericci, L., Vanzella, E., Fontana, A., et al. 2014, ApJ, 793, 113
Pettini, M., & Pagel, B. E. J. 2004, MNRAS, 348, L59
Pettini, M., Rix, S. A., Steidel, C. C., et al. 2002, ApJ, 569, 742
Rigby, J. R., Bayliss, M. B., Gladders, M. D., et al. 2014, ApJ, 790, 44
Rigby, J. R., Wuyts, E., Gladders, M. D., Sharon, K., & Becker, G. D. 2011, ApJ, 732, 59
Schaerer, D., Contini, T., & Pindao, M. 1999, A&AS, 136, 35
Shapley, A. E., Steidel, C. C., Pettini, M., & Adelberger, K. L. 2003, ApJ, 588, 65
Smail, I., Swinbank, A. M., Richard, J., et al. 2007, ApJL, 654, L33
Stark, D. P., Richard, J., Charlot, S., et al. 2015, MNRAS, 450, 1846
Stark, D. P., Richard, J., Siana, B., et al. 2014, MNRAS, 445, 3200
Tilvi, V., Papovich, C., Finkelstein, S. L., et al. 2014, ApJ, 794, 5
Treu, T., Schmidt, K. B., Trenti, M., Bradley, L. D., & Stiavelli, M. 2013, ApJL, 775, L29
Treu, T., Trenti, M., Stiavelli, M., Auger, M. W., & Bradley, L. D. 2012, ApJ, 747, 27
Verhamme, A., Orlitová, I., Schaerer, D., & Hayes, M. 2015, A&A, 578, A7
Whitaker, K. E., Rigby, J. R., Brammer, G. B., et al. 2014, ApJ, 790, 143
Wuyts, E., Barrientos, L. F., Gladders, M. D., et al. 2010, ApJ, 724, 1182
Wuyts, E., Rigby, J. R., Gladders, M. D., et al. 2012a, ApJ, 745, 86
Wuyts, E., Rigby, J. R., Gladders, M. D., & Sharon, K. 2014, ApJ, 781, 61
Wuyts, E., Rigby, J. R., Sharon, K., & Gladders, M. D. 2012b, ApJ, 755, 73